Stopped-Flow Studies of the Mechanisms of Ozone–Alkene Reactions in the Gas Phase. Ethylene

John T. Herron* and Robert E. Huie

Contribution from the Institute for Materials Research, National Bureau of Standards, Washington, D.C. 20234. Received January 10, 1977

Abstract: The reaction of ozone with ethylene has been studied in the gas phase at 298 K and 1.1 kPa (8 Torr), using a stopped-flow reactor coupled to a beam-sampling mass spectrometer. The concentrations of C_2H_4 and the products CO_2, H_2O, CH_2O, HCOOH, CH_3OH, and an unidentified product at mass 43 were measured as a function of reaction time. Using a computer model, the role of free radicals in the reaction was quantitatively assessed, and a complex free-radical mechanism proposed. The initial reactions occurring are postulated to be: $C_2H_4 + O_3 \rightarrow CH_2O + CH_2O_2$; $CH_2O_2 \rightarrow [HCOOH]^\dagger \rightarrow H_2O + CO$ (67%); $CH_2O_2 \rightarrow [HCOOH]^\dagger \rightarrow H_2 + CO_2$ (18%); $CH_2O_2 \rightarrow [HCOOH]^\dagger \rightarrow 2H + CO_2$ (9%); $CH_2O_2 \rightarrow [HCOOH]^\dagger \rightarrow$ (M?, wall?) HCOOH (6%). If these results hold under atmospheric conditions, they imply that considerably fewer free radicals are produced in the reactions of ozone with terminal alkenes than previously assumed.

The role of ozone in photochemical smog has been treated in detail by Leighton[1] and Demerjian, Kerr, and Calvert.[2] As these studies indicate, ozone–olefin reactions are among the most important of all classes of atmospheric chemical reactions. For the purposes of atmospheric modeling, it is necessary to know the rate constants and the primary product yields of these reactions under atmospheric conditions. Although there is now basic agreement on the rate constants for these reactions, there remains considerable uncertainty as to their mechanisms, mostly because of the lack of reliable data on the temporal behavior of reactants and products.

In this paper, we present data on the product yields of the ozone–ethylene reaction obtained as a function of reaction time, from which a detailed reaction mechanism is derived.

Experimental Section

The reaction was studied using a combination of a stopped-flow reactor and a beam-sampling mass spectrometer. This apparatus was used previously by us in measuring rate constants for reactions of ozone with alkenes.[3,4] The configuration of the apparatus used in the present work is shown in Figure 1.

The reactor was a 300-cm³ bulb, jacketed for temperature control, equipped with solenoid valves on the inlet and outlet ports. A gas sample from the reactor was leaked continuously into the mass spectrometer through a 125-μm orifice.

The ozone, produced at about a 5% yield in pure O_2 using a commercial ozonizer, was flowed directly into the reactor at a total pressure of 1.1 kPa (8 Torr). Ethylene was added to the ozone stream just ahead of the solenoid valve on the inlet side of the reactor at a partial pressure between 5 and 10% that of ozone.

The quadrupole mass spectrometer used in this work originally employed electron impact ionization, but for the present work was converted to photoionization, which has the advantage of reducing the complexity of the mass spectrum of the multicomponent systems encountered in this work.[5] The photoionization sources used were argon or helium resonance lamps constructed according to the design of Gorden, Rebbert, and Ausloos.[6] They were mounted on flanges with the lamp windows coming to about 0.75 in. of the ion source chamber. Four 0.375-in. holes were drilled into the ion source chamber to allow the radiation to pass through. A disk with a 0.25-in. hole located 1/16 in. from the ion source chamber was used to collimate the light from the resonance lamp. Light passing through the ion source was monitored by means of a copper detector.

Photoionization sources are less intense than electron impact sources and thus require more sensitive detection techniques. The use of conventional Cu–Be dynode type particle detectors in conjunction with ion counting was not possible in our experiments because of a severe noise problem associated with pickup of the rf voltages applied to the quadrupole. Instead, a Daly detector was used,[7] consisting of a stainless steel knob plated with aluminum and held at −30 kV and a plastic scintillation detector coated with a thin layer of aluminum and held at ground potential. Ions from the mass analyzer strike the knob and eject electrons which are then accelerated toward the scintillator.

The resulting light pulse is detected by a phototube, amplified, and fed into a discriminator which filters out low level noise, including single photon events (from scattered light). The pulses from the discriminator are fed into a scaler or into a multichannel analyzer which allows a mass spectrum to be taken or the temporal behavior of a single mass peak to be followed.

In an experiment, conditions were adjusted as desired and the mass spectrometer focused to a single reactant or product peak. The valves on the reactor were closed simultaneously, which also initiated the sweep of the multichannel analyzer. At the same time, a by-pass valve opened to divert the flow of reacting gases around the reactor to the pump. This process could be repeated as many times as necessary to accumulate adequate data. The data were transferred from the analyzer via a teletype to a time-shared computer for subsequent data reduction and analysis using linear or nonlinear least-squares programs.

Calibration was carried out by preparing gas mixtures and admitting them to the reactor at the same pressure as was used in the experiments. For formaldehyde, acetaldehyde, and acetic acid the reactive gas generator of Walker and Tsang[8,9] was used. This permitted us, for example, to generate an equimolar mixture of formaldehyde and propene from the pyrolysis of allyl methyl ether. Knowing the sensitivity of propene in independent measurements leads directly to a value for formaldehyde. Formic acid was not calibrated for, and the value used to derive the concentrations given below was that of acetic acid. Likewise, the peak at mass 43 was arbitrarily assigned the same sensitivity as formic acid to make qualitative comparisons possible.

Results

With an argon resonance lamp (11.6, 11.8 eV), the largest product peak was found at mass 30, corresponding to formaldehyde. Less intense peaks were observed at mass 46, corresponding to formic acid, and masses 32 and 43. No attempt was made to identify every possible product peak. Minor peaks at masses 33, 34, 42, 44, 60, 62, and 64 were found, but the temporal behavior of these product species was not studied. No signal was found at mass 76 corresponding to the ozonide.

Using a He resonance lamp (21.2 eV), additional peaks at mass 18 (water) and 44 (carbon dioxide) appeared. A peak was also observed at mass 28 corresponding to the expected product, carbon monoxide. However, contributions at mass 28 by ethylene and nitrogen (from an air leak) made quantitative measurement impossible. Hydrogen, another probable product, could not be measured in the apparatus as it was employed.

The temporal behavior of the mass peaks after closing the valves in the stopped-flow reactor was monitored using the multichannel analyzer. Typical data are shown in Figure 2. In Figures 3 and 4, the smoothed data are presented in concentration units. Note that in these curves, and in all of our data, there exists a decay component, having a first-order rate constant of about 2.5×10^{-3} s, due to pump out of the contents of the reactor through the sampling orifice.
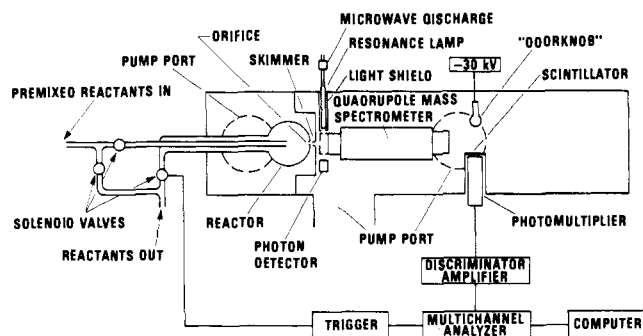
Figure 1. Stopped-flow reactor and beam-sampling mass spectrometer. The total length of the vacuum chamber is about 1.05 m.
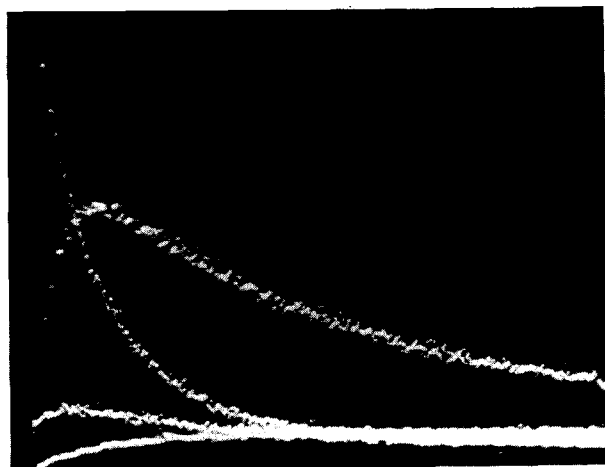

Figure 2. Ozone-ethylene reaction. Typical data set, showing decay of ethylene, and formation of products formaldehyde, mass 32, and formic acid (in that order, going down left hand side of figure). Data set is the result of a single sweep over a 500-s time interval using an argon resonance lamp. $[O_3]_0 = 1.93 \times 10^{-8}$ mol cm^{-3}. $[C_2H_4]_0 = 1.39 \times 10^{-9}$ mol cm^{-3}. $[O_2]_0 = 4.08 \times 10^{-7}$ mol cm^{-3}.

The peak at mass 32 is difficult to interpret. Some signal is observed there in the absence of reaction, which is probably due to ionization of molecular oxygen by photoelectrons. The bulk of the signal, however, probably is due to methanol and $O_2(^1\Delta_g)$. The presence of methanol was verified by gas chromatography and by isotopic substitution experiments using C_2D_4. In the latter experiment, the yield of CD_3OD was considerably smaller than that of mass 32 from the C_2H_4 experiments. The yield measured in the C_2D_4 experiment is an upper limit since products such as D_2O_2 have the same mass.

Discussion

Attempts to fit the data to functions representing simple first-order buildup of products, with correction for effusion, were not successful, indicating that secondary reactions produce or consume the primary products, leading to a more complex functional form for the product behavior. The behavior of the products can be understood better from an analysis of the yield curves, shown in Figure 5. Here, the product yield (amount of product divided by the amount of ethylene consumed) is plotted against reaction time. It is apparent from this figure that formaldehyde is being consumed as the reaction proceeds, probably due to a secondary reaction. In addition, water, carbon dioxide, and formic acid are being produced in secondary reactions.

By extrapolating these yield curves to $t = 0$, a "zero time" reaction stoichiometry can be obtained. This is not necessarily the same as the stoichiometry of the initial reaction since some secondary reactions, especially those involving H, OH, and
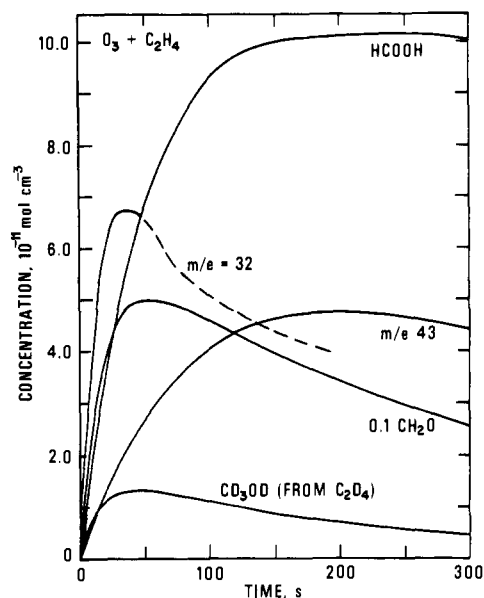

Figure 3. Ozone-ethylene reaction. Temporal behavior observed using an argon resonance lamp. $[O_3]_0 = 1.93 \times 10^{-8}$ mol cm^{-3}. $[C_2H_4]_0 = 1.39 \times 10^{-9}$ mol cm^{-3}. $[O_2]_0 = 4.08 \times 10^{-7}$ mol cm^{-3}.
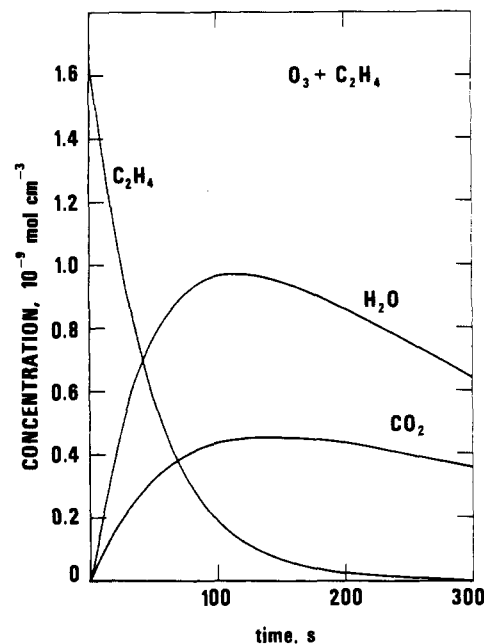

Figure 4. Ozone-ethylene reaction. Temporal behavior observed using a helium resonance lamp. $[O_3]_0 = 2.10 \times 10^{-8}$ mol cm^{-3}. $[C_2H_4]_0 = 1.72 \times 10^{-9}$ mol cm^{-3}. $[O_2]_0 = 4.08 \times 10^{-7}$ mol cm^{-3}.

HO_2, may occur so fast that they are virtually instantaneous on our time scale. The effects of slow secondary reactions, however, are eliminated.

From Figure 5, the $t = 0$ stoichiometry is

$$1.0C_2H_4 \rightarrow 1.0CH_2O + 0.67H_2O + 0.27CO_2$$
$$+ 0.06HCOOH + 0.03CD_3OD \text{ (from } C_2D_4)$$
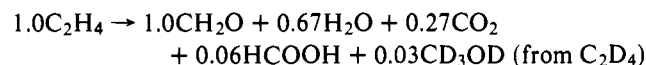
From this stoichiometry, we obtain a 68% carbon balance and a 90% hydrogen balance. (The amount of ozone consumed is not measured in our experiments.)

The observation that one formaldehyde is produced for each ethylene consumed lends support to the conclusion that the reaction proceeds as in solution, via the Criegee split.[10]
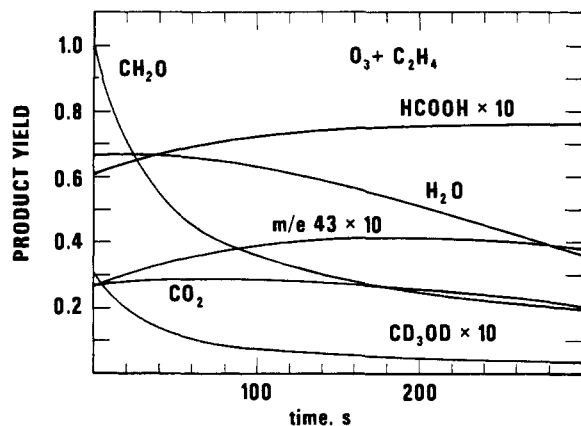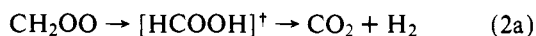
$$O_3 + C_2H_4 \rightarrow CH_2O + CH_2OO \qquad (1)$$

Herron, Huie / Ozone-Ethylene Reactions in the Gas Phase
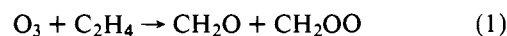
Figure 5. Product yield (Δ product/Δ ethylene) as a function of reaction time. Based on data from Figures 3 and 4. Note that no correction for pump-out has been made.

The methylene peroxide, CH_2OO, is known to undergo secondary reactions in solution leading to the formation of secondary ozonides. In the gas phase, it is more likely to decompose. Wadt and Goddard[11] have suggested that it can rearrange to a "hot" acid and then decompose:

$$CH_2OO \rightarrow [HCOOH]^\dagger \rightarrow CO_2 + H_2 \qquad (2a)$$

$$\rightarrow CO + H_2O \qquad (2b)$$

$$\xrightarrow[\text{wall?}]{M?} HCOOH \qquad (2c)$$

If this is correct, then the amount of hydrogen produced in the reaction equals the amount of carbon dioxide and the amount of carbon monoxide produced equals the amount of water. If these additional products are taken into account, then the carbon balance becomes 102% and the hydrogen balance 103%. (Minor products, including the one identified as mass 43, are not included in this calculation.)
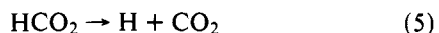
In studies of the chemiluminescence of the ozone-ethylene reaction, Meinel band emission was observed,[12] which is known to arise from the reactions

$$H + O_3 \rightarrow OH^\dagger + O_2 \qquad (3)$$

$$OH^\dagger \rightarrow OH + h\nu \qquad (4)$$
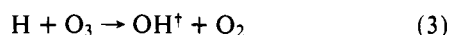
The atomic hydrogen could be formed from an additional decomposition mode of the excited formic acid:

$$[HCOOH]^\dagger \rightarrow H + HCO_2 \qquad (2d)$$

followed by

$$HCO_2 \rightarrow H + CO_2 \qquad (5)$$
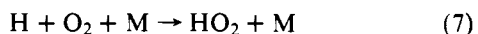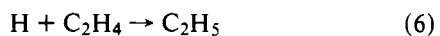
This additional decomposition mode does not affect the corrected carbon or hydrogen balances.

Under conditions $O_3 > C_2H_4$, and at low pressure, the competing hydrogen atom reactions

$$H + C_2H_4 \rightarrow C_2H_5 \qquad (6)$$

$$H + O_2 + M \rightarrow HO_2 + M \qquad (7)$$

are not important.

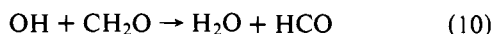Hydroxyl radicals produced in eq 3 can react with ethylene, ozone, formaldehyde, or carbon monoxide:

$$OH + C_2H_4 \rightarrow C_2H_4OH \qquad (8)$$

$$OH + O_3 \rightarrow HO_2 + O_2 \qquad (9)$$

$$OH + CH_2O \rightarrow H_2O + HCO \qquad (10)$$
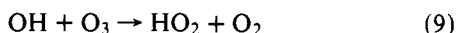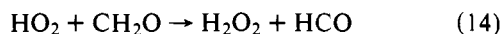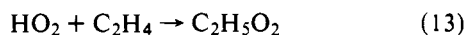
$$OH + CO \rightarrow H + CO_2 \qquad (11)$$

Table I. Mechanism of the Ozone-Ethylene Reaction at Low Pressure

Reaction	Rate constant, $cm^3\ mol^{-1}\ s^{-1}$ [a]
(1) $O_3 + C_2H_4 \rightarrow CH_2O + CH_2OO$	1.0×10^6
(2a) $CH_2OO \rightarrow [HCOOH]^\dagger \rightarrow CO_2 + H_2$	18%
(2b) $CH_2OO \rightarrow [HCOOH]^\dagger \rightarrow CO + H_2O$	67%
(2d) $CH_2OO \rightarrow [HCOOH]^\dagger \rightarrow H + HCO_2$	9% [b]
(2c) $CH_2OO \rightarrow [HCOOH]^\dagger \rightarrow HCOOH$	6%
(5) $HCO_2 \rightarrow H + CO_2$	[b]
(3) $H + O_3 \rightarrow OH + O_2$	1.6×10^{13}
(6) $H + C_2H_4 \rightarrow C_2H_5$	2.3×10^{11} [c]
(8) $OH + C_2H_4 \rightarrow C_2H_4OH$	2.0×10^{12}
(9) $OH + O_3 \rightarrow HO_2 + O_2$	2.8×10^{10}
(10) $OH + CH_2O \rightarrow H_2O + HCO$	8.4×10^{12}
(12) $HO_2 + O_3 \rightarrow OH + 2O_2$	9.0×10^8
(15) $HCO + O_2 \rightarrow HO_2 + CO$	3.4×10^{12}
(16) $HCO + O_3 \rightarrow HCO_2 + O_2$	3.4×10^{12} [d]
(17) $HO_2 + HO_2 \rightarrow H_2O_2 + O_2$	3.4×10^{12}
(18) $C_2H_5 + O_2 \rightarrow C_2H_5O_2$	1×10^{11} [d]
(19) $C_2H_5 + O_3 \rightarrow CH_2O + CH_3 + O_2$	5.5×10^{11} [d]
(20) $CH_3 + O_2 \rightarrow CH_3O_2$	3×10^{10} [e]
(21) $CH_3 + O_3 \rightarrow CH_2O + H + O_2$	5.5×10^{11} [f]
(22) $C_2H_4OH + O_2 \rightarrow C_2H_4(OH)O_2$	1×10^{11} [d]
(23) $C_2H_4OH + O_3 \rightarrow CH_2O + CH_2OH + O_2$	5.5×10^{11} [d]
(24) $CH_2OH + O_2 \rightarrow CH_2(OH)O_2$	1×10^{11} [d]
(25) $CH_2OH + O_3 \rightarrow CH_2O + OH + O_2$	5.5×10^{11} [d]
(26) $RO_2 + RO_2 \rightarrow O_2 + product$	1×10^{11} [g]
(27) $HO_2 + RO_2 \rightarrow O_2 + product$	1×10^{11} [d]

[a] All rate constants from ref 21, except as noted. [b] Assumed to be very fast. [c] Reference 22. [d] Estimated. [e] Reference 23. The minor path $CH_3 + O_2 \rightarrow CH_2O + OH$ is neglected. Note that this rate constant is uncertain to a factor of at least 2. [f] Reference 24. [g] Estimated: see ref 25.
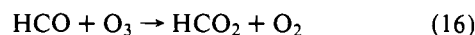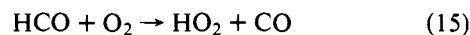
Reaction 11 is not important under our conditions but reactions 8, 9, and 10 probably are.

The hydroperoxyl radical can react with ozone, ethylene, or formaldehyde:

$$HO_2 + O_3 \rightarrow OH + 2O_2 \qquad (12)$$

$$HO_2 + C_2H_4 \rightarrow C_2H_5O_2 \qquad (13)$$

$$HO_2 + CH_2O \rightarrow H_2O_2 + HCO \qquad (14)$$
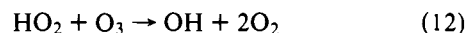
Probably only the reaction with ozone is of any importance.

Formyl radicals can react with oxygen or ozone:

$$HCO + O_2 \rightarrow HO_2 + CO \qquad (15)$$

$$HCO + O_3 \rightarrow HCO_2 + O_2 \qquad (16)$$

Reaction 16 is speculative and has been assigned the same rate constant as 15. It has been inferred from studies at higher pressures that the association reaction of HCO with O_2 is important.[26] In a study at lower pressure, comparable to that used in this work, no evidence for this reaction was found.[27] Therefore, the association reaction was not included in the mechanism used here.

This sequence of reactions forms a chain for the decomposition of ozone which can be terminated by

$$HO_2 + HO_2 \rightarrow H_2O_2 + O_2 \qquad (17)$$
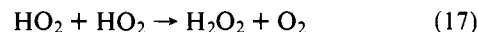
These reactions (with a few of the less important ones omitted) are given in the first part of Table I. The rate constants for this limited set of reactions are, for the most part, well established and their values included in Table I. The major unknown is the ratio k_{2a}/k_{2d}. The sum $k_{2a} + k_{2d}$ is known from the yield of carbon dioxide at time zero. Similarly, the fraction of decomposition of the methylene peroxide leading
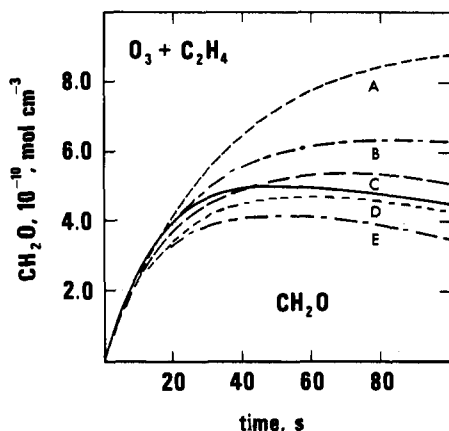
Figure 6. Comparison of observed (solid line) and calculated (dashed lines) formaldehyde profiles in the ozone-ethylene reaction. for k_{2a}/k_{2d} = (A) ∞, (B) 4, (C) 2, (D) 1, and (E) 0.5.

Figure 7. Comparison of observed (solid lines) and calculated (dashed lines) water and carbon dioxide profiles in the ozone-ethylene reaction.

to water and formic acid was taken from the corresponding yields of these products at time zero. In order to derive the ratio k_{2a}/k_{2d}, it was observed that in the proposed mechanism, formaldehyde was lost only through reaction with hydroxyl radicals. In turn, the hydroxyl radical concentration depends on the number of hydrogen atoms produced in reaction 2d (and the subsequent reaction 5). Therefore, it should be possible to calculate from the behavior of formaldehyde the hydrogen atom production rate from reactions 2d and 5. This was done by modeling the system using a computer program developed by Brown,[13] based on the Gear method[14] for handling "stiff" systems. Initially, only reactions through number 17 in Table I were included. Various values of the branching ratio k_{2a}/k_{2d} were used and the best fit of the projected formaldehyde concentration profile to the experimental data was sought. This was found at k_{2a}/k_{2d} = 2.

Although the reactions considered above are the most important under our experimental conditions, additional reactions are necessary to account for the fate of the radicals produced in reactions 6 and 8, and to account for the behavior of the system under different experimental conditions. Unfortunately, there is not much information available on the kinetics or mechanisms of these reactions and certain assumptions were necessary. It was assumed that all alkyl-type radicals react only with oxygen or ozone and that hydroxyalkyl radicals behave the same as alkyl radicals. On this basis we arrived at reactions 18-25 in Table I. In addition, we included the radical-radical termination reactions, 26 and 27.

Using this extended set of reactions, and the ratio k_{2a}/k_{2d} = 2, the calculation was rerun. Only a slight change in the formaldehyde profile resulted. The calculations were then run using ratios k_{2a}/k_{2d} = 4, 1, and 0.5. These profiles along with the experimental data are given in Figure 6. The runs were limited to the first 100 s of reaction time, at which point 90% of the ethylene was consumed. At longer times, slow secondary reaction paths not included in our model probably become important. Our choice of k_{2a}/k_{2d} = 2 as the best fit to the data is subject to considerable uncertainty, and values lying between k_{2a}/k_{2d} = 1 to 3 cannot be ruled out.

Carbon dioxide and water profiles predicted by the model are compared with observation in Figure 7. The fit to the water data is excellent, but the carbon dioxide data fit well only at short reaction times. At longer times, it falls short of the observations, suggesting an additional major source of carbon dioxide. Obviously the mechanism used to model our data is far from complete, accounting only for the major reaction products. It does not account for methanol, the bulk of the formic acid, or the peak at mass 43.

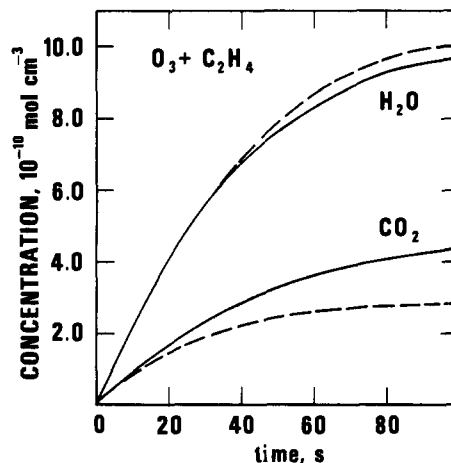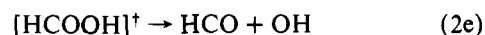An additional decomposition mode for the excited formic

acid, from the rearrangement of the methylene peroxide, is possible:

$$[HCOOH]^\dagger \rightarrow HCO + OH \qquad (2e)$$

As with reaction 2d (followed by reaction 5) this reaction produces two active radicals and would not be expected to lead to much change in the model predictions. This was tested by substituting reaction 2e for 2d and rerunning the calculations. The changes in major product and the reactant curves were insignificant. Since there is independent evidence for the production of hydrogen atoms in the ozone-ethylene reaction and since the inclusion of reaction 2e makes no difference in the model predictions for those species monitored, we have chosen to exclude this reaction at this time.

In principle it should be possible to compare the predictions of the mechanism presented here with the observations of other workers. Unfortunately, little of that information is in a form suitable for this purpose. Toby, Toby, and O'Neal,[15] however, have measured the decay of ozone at low total pressure, under conditions of excess ethylene, with and without oxygen initially present. With excess oxygen, the ozone decay was first order, but with no oxygen initially present, the ozone decay was much faster and clearly not first order. We have taken their data for a system initially free of oxygen and used our mechanism to predict the concentration profiles of oxygen and ozone. As shown in Figure 8, the fit is excellent. It is apparent that the buildup of molecular oxygen is very fast and the system, after a few seconds, passes from being oxygen free to one in which the concentration of oxygen exceeds that of ozone. The predicted ratio of oxygen formed to ozone consumed at extended reaction times is about 0.4, in apparent agreement with the observations of Toby et al.[15] They find, however, that as the ozone concentration increases, the yield of oxygen (O_2 produced/O_3 consumed) approaches 1.5. Our mechanism does not predict a yield much in excess of 0.5 under any experimental condition. In fact, it is difficult to conceive of any mechanism other than a thermal decomposition which could lead to such a high yield of oxygen.

Two other studies on the reaction at low pressures are relevant to the present work. Kühne, Vaccani, Ha, Bauder, and Günthard[16] studied the reaction using combinations of infrared matrix spectroscopy, mass spectrometry, and microwave spectroscopy. These workers report on relative product yields from a mixture of 2 Torr each of ethylene and ozone reacted over a 30-s period. Their results are given in Table II along with the values predicted by the model. The agreement is not satisfactory. There are, however, some very severe experimental problems in the work of Kühne et al. which make their data highly suspect. First, the reaction time is based on experiments
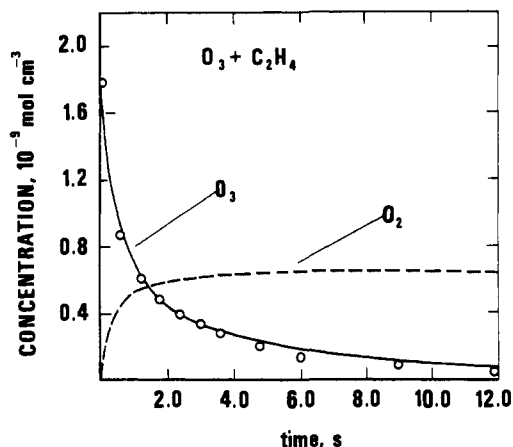
Figure 8. Comparison of observed (open circles) and calculated (solid line) ozone profiles in the ozone–ethylene reaction. Also shown is the predicted oxygen profile. $[C_2H_4]_0 = 1.30 \times 10^{-7}$ mol cm^{-3}. $[O_3]_0 = 1.77 \times 10^{-9}$ mol cm^{-3}. $[O_2]_0 = 0$. Data of Toby, Toby, and O'Neal.[15]

Table II. Product Analysis after 30 s Reaction Time of 10^{-7} mol cm^{-3} Each of C_2H_4 and O_3 (Data of Kühne et al.[16])

Species	% of total pressure observed	% of total pressure predicted
O_3	10	1.3
C_2H_4	25	24
H_2O	4	14
CH_2O	6	18
HCOOH	1	0.9
CH_3OH	0.02	
CH_3CHO	0.2	
CH_2OCH_2	0.1	
$(CHO)_2O$	0.2	
CH_2OHCHO	0.04	
Remainder (mainly CO, O_2, CO_2)	53.44	
CO		10
CO_2	41.8	6.2
H_2		2.6
O_2		23

using a linear flow reactor (of unspecified dimensions) at a total pressure of 4 Torr. It is not possible for a flow reactor to exhibit anything approaching plug flow at these pressures and the low flow rates needed to have a 30-s reaction time. Aside from this the question of analytical accuracy, especially in view of the demonstrated wall effects, is not satisfactorily addressed. Specifically, it is not possible to obtain a consistent elemental balance from their reported yields. We therefore doubt that these data have quantitative value. Qualitatively, however, they observe that in experiments using the waveguide cavity as a reactor the principal products, carbon monoxide, carbon dioxide, formaldehyde, and water, are formed rapidly while other products such as ethylene oxide and acetaldehyde are formed over a longer time period, which suggests that they are formed in slower secondary processes. At extremely long reaction times they detect the secondary ozonide. An additional source of minor products in their experiments are wall reactions, particularly those which could occur in the waveguide of the microwave spectrometer.

The other low-pressure study of interest is that of Atkinson, Finlayson, and Pitts,[17] who used photoionization mass spectrometry in conjunction with a flow system to identify reaction products. The only products detected in the ethylene reaction were formaldehyde and a product at mass 43. (Resonance lamps of energies greater than 11.8 eV were not used.) The mass 43 peak was monitored using a xenon resonance lamp with a sapphire window which limits the radiation to the 8.43-eV line. Since the signal increased and then appeared to approach a steady state, and since the species obviously has a low appearance potential, Atkinson et al. suggested that the peak corresponded to the CH_3CO radical. Our concentration profile for mass 43, however, suggests a species that is more stable chemically. It is possible, however, that using an argon resonance lamp, as we did, the peak at mass 43 is mostly a fragment ion whereas with a xenon lamp it is due only to a free radical. In a later study, we hope to explore this problem further.

There also exists a considerable body of data on the ozone–ethylene reaction obtained at atmospheric pressure. Extension of our model to high pressure, however, is difficult. Simple addition reactions such as 8 will become faster, while others such as 5 may lead to different products, i.e., a peroxylformyl radical instead of atomic hydrogen and carbon dioxide. Fortunately, most radicals under atmospheric conditions will be scavenged by oxygen.

Scott, Stephens, Hanst, and Doerr[1,18] measured the products of the reaction of 32 ppm each of ethylene and ozone in 1 atm of oxygen using long-path infrared spectroscopy. They reported

28 ± 10 ppm H_2O, 17 ± 4 ppm CH_2O, 4 ± 1 ppm CO_2, 28 ± 6 ppm CO, and less than 1 ppm HCOOH. In order to model this reaction, it was necessary to reassign rate constants for the pressure-dependent reactions, and to include reaction 7, for which we used $k_7 = 8.2 \times 10^{11}$ cm^3 mol^{-1} s^{-1}. The program was run to 5000 s, where the model predicted the product concentrations 19 ppm H_2O, 24 ppm CH_2O, 7 ppm CO_2, 17 ppm CO, and 1.5 ppm HCOOH. The model also predicted that $\Delta O_3 / \Delta C_2H_4 = 1.07$, whereas Scott et al. found a value of 1.1 when the initial concentrations of ozone and ethylene were each 20 ppm.

The detection of less CH_2O than predicted and more H_2O and CO suggests that either there is an additional source of radicals which is important at high O_2 pressure, or that some additional reactive species are being produced at long times. The prediction of too much CO_2 by the model is surprising, especially since too little is predicted for the present experiments. In general, however, the agreement is satisfactory considering the uncertainty in both measurements and model.

Vrbaski and Cvetanovic[19] measured reaction products for many ozone–alkene reactions using gas chromatography. Unfortunately, most of the important products in the ethylene reaction were not measured. With very high initial reactant concentrations (2×10^{-6} mol cm^{-3} C_2H_4 and 5×10^{-7} mol cm^{-3} O_3) in 1.8×10^{-5} mol cm^{-3} O_2, 1 mol of ozone was reported to yield 0.25 mol of HCOOH and 0.019 mol of CH_3CHO. It seems likely that at these high reactant concentrations, a very substantial portion of the reaction would proceed through free-radical reactions and the CH_3CHO is probably formed from one or more of these secondary reactions. The high yield of HCOOH is probably also a consequence of secondary reactions, some of which may have occurred in the GC column.

In a recent paper, Japer, Wu, and Niki[20] reported on the effect of O_2 on the kinetics of ozone–alkene reactions. The reactants were mixed in the 1–100-ppm range in the presence of an atmosphere of air or helium. For ethylene, the apparent rate constant for ozone decay increased by 38% going from air to helium. We have modeled the reaction in helium, assuming a 0.75-ppm level of O_2 as an impurity, and found that the rate of loss of ozone is accelerated, but also that the first-order plot of ln O_3 against time is curved, so that we cannot derive a true rate constant for comparison with the rate constants given by Japar et al.
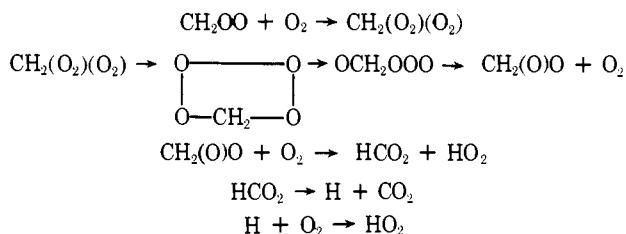
In the above, we have attempted to fit the existing data on

the ozone-ethylene reaction to a model based solely on our observations of the reaction at 1.1 kPa. Obviously, this attempt has been only partially successful since it requires a knowledge of reaction mechanism, reaction rate constants, the effects of total pressure on both mechanism and rate constant, and a reliable body of observation on the temporal behavior of the system. It is possible to adjust rate constants to make the predictions of the model agree better with the observations of other workers. This, in our opinion, is an incorrect procedure. It is preferable to use the model and its predictions as a basis for establishing experimental priorities. The most obvious need is for reliable data on the temporal behavior of the system under atmospheric conditions. In addition, however, greater accuracy of input kinetic data is needed. The ratio k_{12}/k_{17} is a crucial number in determining the OH concentration in the system. Also, much of the uncertainty in the model at extended reaction times arises from ignorance of the secondary chemistry. For example, we do not know the mechanism of reaction of OH with C_2H_4, the nature of the product formed when $C_2H_4 \cdot OH$ reacts with O_2, or how this in turn behaves. We can speculate that some, if not most, of the minor products observed in the gas-phase ozone-olefin reactions arise from hydroxyl radical reactions.

Implications for Atmospheric Chemistry. Most detailed atmospheric chemistry models use propylene or one of the butenes as a starting reactant. All terminal olefins, however, will give rise to a common carbene peroxide, CH_2OO, in their reactions with ozone:

$$R_1R_2C\!\!=\!\!CH_2 + O_3 \rightarrow R_1R_2COO + CH_2O$$

$$\rightarrow R_1R_2CO + CH_2OO$$
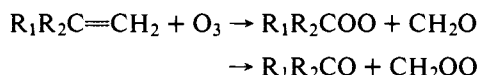
Subsequently it is assumed that the CH_2OO species reacts in the atmosphere to give rise to one or more free radicals per CH_2OO consumed. For example, in the scheme used by Demerjian et al.[2] each CH_2OO leads ultimately to two HO_2 radicals.

$$CH_2OO + O_2 \rightarrow CH_2(O_2)(O_2)$$

$$CH_2(O_2)(O_2) \rightarrow \begin{array}{c} O\!\!-\!\!\!-\!\!\!-\!\!\!-O \\ | \quad\quad | \\ O\!\!-\!\!CH_2\!\!-\!\!O \end{array} \rightarrow OCH_2OOO \rightarrow CH_2(O)O + O_2$$

$$CH_2(O)O + O_2 \rightarrow HCO_2 + HO_2$$

$$HCO_2 \rightarrow H + CO_2$$

$$H + O_2 \rightarrow HO_2$$

Our results, to the extent to which they are applicable at atmospheric pressure, predict a considerably smaller number of radical products; each CH_2OO leads only to 0.2 free radicals.

In many ways, our results confirm the earlier conclusions of Scott et al.[18] that the principal fate of methylene peroxide is decomposition to molecular products. Our results add to that mechanism by allowing for a minor free-radical decomposition path which explains many of the diverse observations in this system.

Summary

1. The primary products of the reaction of ozone with ethylene in the gas phase at low pressure are equal amounts of formaldehyde and methylene peroxide, CH_2OO.

2. Methylene peroxide, under these conditions, decomposes about 90% to molecular products, and about 10% to free-radical products.

3. Free radicals produced by the decomposition of methylene peroxide react with ozone, ethylene, and formaldehyde resulting in a complex but well-defined system which can be treated by computer modeling.

4. The results of these studies, if applicable to real atmospheres, imply that less "active" products are formed in this reaction than can be inferred on the basis of current atmospheric models.

References and Notes

(1) P. A. Leighton. "Photochemistry of Air Pollution". Academic Press. New York, N.Y., 1961.
(2) K. L. Demerjian, J. A. Kerr, and J. G. Calvert. Adv. Environ. Sci. Technol., 4, 1 (1974).
(3) J. T. Herron and R. E. Huie. J. Phys. Chem., 78, 2085 (1974).
(4) R. E. Huie and J. T. Herron. Int. J. Chem. Kinet., Symp. No. 1, 165 (1975).
(5) J. T. Herron. Adv. Mass Spectrom., 5, 453 (1971).
(6) R. Gordon, Jr., R. E. Rebbert, and P. Ausloos. "Rare Gas Resonance Lamps". National Bureau of Standards, Technical Note 496, U.S. Government Printing Office, Washington, D.C., 1969.
(7) N. R. Daly. Rev. Sci. Instrum., 31, 264 (1960).
(8) J. A. Walker and W. Tsang. "The Construction, Operation, and Performance of a Reactive Gas Generator; with Specific Application to HCHO, CH₃CHO, CH₂CHCHO, SO₂, HCN and HCl Production", National Bureau of Standards, Interim Report NBSIR 76-1000, 1976.
(9) W. Tsang and J. A. Walker. Anal. Chem., 49, 13 (1977).
(10) R. Criegee. Angew. Chem., Int. Ed. Engl., 14, 745 (1975).
(11) W. R. Wadt and W. A. Goddard, III. J. Am. Chem. Soc., 97, 3004 (1975).
(12) B. J. Finlayson, J. N. Pitts, Jr., and R. Atkinson. J. Am. Chem. Soc., 96, 5356 (1974).
(13) R. L. Brown. "A Computer Program for Solving Systems of Chemical Rate Equations", National Bureau of Standards, Interim Report NBSIR 76-1055. in press.
(14) C. W. Gear. "Numerical Initial Value Problems in Ordinary Differential Equations", Prentice-Hall, Englewood Cliffs. N.J., 1971.
(15) F. S. Toby. S. Toby, and H. E. O'Neal. Int. J. Chem. Kinet., 8, 25 (1976).
(16) H. Kühne, S. Vaccani, T.-K. Ha, A. Bauder, and H. H. Günthard. Chem. Phys. Lett., 38, 449 (1976).
(17) R. Atkinson. B. J. Finlayson, and J. N. Pitts, Jr., J. Am. Chem. Soc., 95, 7592 (1973).
(18) W. E. Scott, E. R. Stephens, P. L. Hanst. and R. C. Doerr, Proc., Am. Pet. Inst., Sect. 3, 37, 171 (1957). These results are also included in ref. 1, p. 168.
(19) T. Vrbaski and R. J. Cvetanovic, Can. J. Chem., 38, 1063 (1960).
(20) S. M. Japar. C. H. Wu, and H. Niki, J. Phys. Chem., 80, 2057 (1976).
(21) R. F. Hampson, Jr., and D. Garvin, Ed., "Chemical Kinetic and Photochemical Data for Modelling Atmospheric Chemistry", National Bureau of Standards, Technical Note 866, U.S. Government Printing Office, Washington, D.C., 1975.
(22) M. J. Kurylo, N. C. Peterson, and W. Braun. J. Chem. Phys., 53, 2776 (1970).
(23) N. Washida and K. D. Bayes. Int. J. Chem. Kinet., 8, 777 (1976).
(24) R. Simonaitis and J. Heicklen, J. Phys. Chem., 79, 298 (1975).
(25) J. Weaver, R. Shortridge, J. Meagher, and J. Heicklen, J. Photochem., 4, 109 (1975).
(26) T. L. Osif and J. Heicklen. J. Phys. Chem., 80, 1526 (1976).
(27) N. Washida, R. I. Martinez, and K. D. Bayes. Z. Naturforsch. A, 29, 251 (1974).